Title: Spatio-temporal brain dynamics mediating post-error behavioral adjustments.
Authors: Manuel AL, Bernasconi F, Murray MM, Spierer L
Journal: Journal of cognitive neuroscience
Year: 2012 Jun
Volume: 24
Issue: 6
Pages: 1331-43
DOI: 10.1162/jocn_a_00150

Spatio-temporal Brain Dynamics Mediating Post-error Behavioral Adjustments

Aurelie L. Manuel[1], Fosco Bernasconi[1], Micah M. Murray[1,2,3], and Lucas Spierer[1,4]

Abstract

■ Optimal behavior relies on flexible adaptation to environmental requirements, notably based on the detection of errors. The impact of error detection on subsequent behavior typically manifests as a slowing down of RTs following errors. Precisely how errors impact the processing of subsequent stimuli and in turn shape behavior remains unresolved. To address these questions, we used an auditory spatial go/no-go task where continual feedback informed participants of whether they were too slow. We contrasted auditory-evoked potentials to left-lateralized go and right no-go stimuli as a function of performance on the preceding go stimuli, generating a 2 × 2 design with "preceding performance" (fast hit [FH], slow hit [SH]) and stimulus type (go, no-go) as within-subject factors. SH trials yielded SH trials on the following trials more often than did FHs, supporting our assumption that SHs engaged effects similar to errors. Electrophysiologically, auditory-evoked potentials modulated topographically as a function of preceding performance 80–110 msec poststimulus onset and then as a function of stimulus type at 110–140 msec, indicative of changes in the underlying brain networks. Source estimations revealed a stronger activity of prefrontal regions to stimuli after successful than error trials, followed by a stronger response of parietal areas to the no-go than go stimuli. We interpret these results in terms of a shift from a fast automatic to a slow controlled form of inhibitory control induced by the detection of errors, manifesting during low-level integration of task-relevant features of subsequent stimuli, which in turn influences response speed. ■

INTRODUCTION

Rapid and flexible adaptation to environmental requirements is critical for optimal goal-directed behaviors. Behavioral adjustments are typically driven by the detection of inappropriate responses, potentially yielding negative consequences (e.g., MacDonald, Cohen, Stenger, & Carter, 2000). The impact of error detection on subsequent behavior typically manifests as a slowing down of RTs following errors as reported in various paradigms including the Stroop task (Egner & Hirsch, 2005), stop signal task (Li et al., 2008), or go/no-go tasks (e.g., Hester, Simoes-Franklin, & Garavan, 2007). Whereas the neural underpinnings of error detection have been the focus of extensive investigations, how it impacts the processing of subsequent stimuli and in turn shapes behavior remains unclear.

Error detection processes have been repeatedly found to involve the ACC (Garavan, Ross, Murphy, Roche, & Stein, 2002) as notably evidenced by higher activity within ACC, following errors than correct responses (e.g., Ullsperger & von Cramon, 2004). ERP studies further revealed that error-related components generated within ACC peak 50–100 msec postresponse onset when the inappropriateness of a response is detected (Dikman & Allen, 2000; Gehring, Goss, Coles, Meyer, & Donchin, 1993). Although still debated, current views hold that error-related activity is elicited by comparison mechanisms between the expected versus actual response outcome (Carter & van Veen, 2007).

Prominent models suggest that, in the case of an error, performance monitoring mechanisms supported by ACC trigger the engagement of antero-lateral prefrontal regions, notably including the dorsolateral pFC (DLPFC). In turn, these areas would mediate behavioral adjustments (e.g., Botvinick, Braver, Barch, Carter, & Cohen, 2001; see also Kerns et al., 2004). Supporting the role of ACC–DLPFC interactions in behavioral adjustment, the activity of ACC has been found to predict both the magnitude of subsequent pFC involvement and the extent of post-error slowing (PES; Kerns et al., 2004; Ridderinkhof, Ullsperger, Crone, & Nieuwenhuis, 2004).

A recent account for PES effects assumes that response speed decreases because participants need to refocus attention to the task following the distraction (Nunez Castellar, Kuhn, Fias, & Notebaert, 2010; Notebaert et al., 2009) or the increase in arousal induced by the occurrence of infrequent, unexpected error trials (Carp & Compton,

[1]Vaudois University Hospital Center and University of Lausanne, [2]Center for Biomedical Imaging, Lausanne, Switzerland, [3]Vanderbilt University Medical Center, Nashville, TN, [4]University of Fribourg, Switzerland

2009; Taylor, Stern, & Gehring, 2007). Alternative, nonexclusive hypotheses advance that PES merely reflects a switch to more conservative response modes, increasing the probability of making a correct response on subsequent trials by favoring accuracy over response speed (Holroyd, Yeung, Coles, & Cohen, 2005; Botvinick et al., 2001). Compatible with these assumptions, converging evidence documents the involvement of DLPFC in modulating the allocation of attention (MacDonald et al., 2000) and in modulating the level of top–down executive control engaged in resolving a task (Ridderinkhof, van den Wildenberg, Segalowitz, & Carter, 2004).

The studies reviewed above demonstrate that errors impact behavioral responses to the subsequent stimulus mediated by interaction between error detection mechanisms comprised within ACC and the consequent increase in executive control or attentional modulation driven by the DLPFC. However, how these processes act on the neurophysiological processing of subsequent stimuli to shape behavior remains unclear.

Recent models of inhibitory control suggest that participants adopt an automatic, controlled response mode once stimulus–response mapping rules are learned. Automatic response mode concerns both responses to go trials and inhibition of motor responses to no-go trials (engagement of no-go goals) and involves a feedforward control of stimulus–response mapping by parieto-prefrontal executive networks over the very initial stages of sensory integration (Manuel, Grivel, Bernasconi, Murray, & Spierer, 2010; Verbruggen & Logan, 2008; Logan, 1988; Shiffrin & Schneider, 1977). As it does not rely solely on slow top–down inputs from frontal executive modules, an automatic response mode allows optimal go/no-go performance consisting in reduced RT to go stimuli while keeping low the rate of false alarms (FAs; Kenner et al., 2010; Manuel et al., 2010). According to this model, it could be predicted that the detection of errors would induce a switch from automatic to more controlled forms of inhibition and increase the level of top–down executive control, in turn slowing down responses.

Most of the previous studies focused on the neural correlates of error detection (i.e., processes related to the commission of the error) and correlated it with subsequent performance and behavioral adjustments (e.g., Kerns et al., 2004; Ridderinkof, Ullsperger, et al., 2004). Consequently, previous literature did not directly distinguish between error detection mechanisms and subsequent behavioral adjustments (e.g., Fiehler, Ullsperger, & von Cramon, 2004; Garavan et al., 2002). For example, Garavan et al. (2002) assessed the brain mechanisms of behavioral adjustments but did not directly focus on how the following stimulus was processed. As another example, Fiehler and colleagues (2004) aimed at distinguishing between error detection and correction. Participants were separated in two groups and were asked to either immediately correct their errors or not. Because they were asked to immediately correct their errors and because error detection precedes error correction in both cases, it seems difficult to evaluate the specific network implicated in behavioral adjustments. However, to our knowledge, only few functional studies on the neural correlates of post-error behavioral adjustment directly addressed how the detection of error affects the processing of subsequent stimuli. Using a stop signal task, Li et al. (2008) examined the brain responses to go trials as a function of the performance to a previous stop stimulus. Their results suggest a role for prefrontal areas, notably the right ventrolateral prefrontal area, in PES. Reinforcement learning studies have also pointed out associations between activity in prefrontal areas and associative learning (Brown & Braver, 2005; Nieuwenhuis, Holroyd, Mol, & Coles, 2004; Holroyd & Coles, 2002), and more specifically, this literature reported associations between error-related activity in pFCs and immediate changes in post-error behavior (Hester, Murphy, Brown, & Skilleter, 2010; Hester, Barre, Murphy, Silk, & Mattingley, 2008; Frank, Woroch, & Curran, 2005; Frank, Seeberger, & O'Reilly, 2004). However, the low temporal resolution of fMRI technique used in their study did not allow for disentangling the precise dynamics of brain mechanisms underlying post-error behavioral adjustments.

To resolve how errors impact the processing of subsequent stimuli to shape behavior, we contrasted electrical neuroimaging analyses of auditory-evoked potentials (AEPs) to stimuli as a function of response performance to the preceding go stimulus recorded during the completion of a speeded auditory spatial go/no-go task, generating a 2×2 design with "preceding performance" (fast hit [FH], slow hit [SH]) and stimulus type (go, no-go) as within-subject factors.

EEG investigations of error-related processes are typically analyzed using response-locked ERPs, notably because error detection processes manifest in time relative to the error commission rather than to the stimulus presentation. Most of the literature focusing on error detection provides convergent evidence for the importance of response-locked error processes during the postresponse period including, for example, the error-related negativity (ERN), N2/P3 components (Dimoska, Johnstone, & Barry, 2006; Falkenstein, Hoormann, Christ, & Hohnsbein, 2000; Falkenstein, Hoormann, & Hohnsbein, 1999; Falkenstein, Koshlykova, Kiroj, Hoormann, & Hohnsbein, 1995; Gehring et al., 1993). The preresponse period has also been shown to comprise indices of FA, indicating that error-related processes manifest before the actual error commission (Pourtois, 2011). However, this study does not focus on error-related processes per se but in how error detection impacts the processing of subsequent stimuli and in turn shapes behavioral adjustments. Therefore, we time-locked the ERP to stimulus onset.

We expect SHs to be processed as error and induce behavioral adjustments for three reason: (i) emphasis was explicitly put on response speed over accuracy, (ii) participants were continuously informed of whether they were too slow by a negative feedback following SHs, and (iii)

SHs were considered as error in the calculation of the global accuracy provided to participants after each trial. In addition, we assessed whether SH induced the typical ERN by averaging response-locked ERP to SH and FH. The former condition indeed showed an ERN, further supporting that SH can be considered as errors in our study. This assumption will be controlled by evaluating if SHs induce PES, that is, the typical post-error behavioral adjustment pattern.

METHODS

Participants

Ten healthy volunteers participated in the study (all men, all right-handed; Oldfield, 1971), aged 22–39 years (mean = 30.10 years, *SD* = 1.53 years). Each participant provided written, informed consent to participate in the study. No participant had a history of neurological or psychiatric illness, and all reported normal hearing. All procedures were approved by the ethics committee of the Faculty of Biology and Medicine of the CHUV and University of Lausanne.

Stimuli

Auditory stimuli were 150 msec noise bursts (200–500 Hz band-pass filtered, 5 msec rise/fall, 44.1 kHz sampling) lateralized by means of a right- or left-ear leading interaural time difference of 770 μsec, which led to perceived lateralization of ca. 80° from the central midline (Blauert, 1997). The sounds were presented via insert earphones (ER-4P; Etymotic Research, Elk Grove Village, IL) at a level judged comfortable by the participant.

Procedure and Task

This study is based on a reanalysis of the data reported in Manuel et al. (2010). Participants underwent an auditory spatial go/no-go task, in which they had to respond as fast as possible via a manual response box button to left-lateralized sounds (go stimuli, hereafter termed LG) and to withhold responses to right-lateralized sounds (no-go stimuli, RNG).

Throughout the experiment, participants were seated in an electrically shielded and sound-attenuated booth in front of a 19-in. LCD screen. Stimulus delivery and response recording were controlled using E-Prime 2.0 (Psychology Tools, Inc., Pittsburgh, PA). Each trial started with the presentation of a visual cue (centrally presented gray cross on a black background) of a randomly determined duration ranging from 1000 to 1900 msec. At the same time that the cross was turned off, the LG or RNG sounds were presented and the time window during which response were recorded was open. LG and RNG trials were presented with an equal probability of .5.

The go/no-go task was divided into three experimental sessions. Each session started with a calibration block of 16 randomly presented trials (8 LG and 8 RNG), followed by two test blocks each of 80 randomly presented trials (40 LG and 40 RNG). The calibration blocks were used to individually adjust the task difficulty and to maintain time pressure across the whole experiment. This was accomplished in the following way. During each calibration phase, the mean RT to LG trials was calculated on-line and used to determine the participant's RT threshold, which was set slightly below current response speed (i.e., calculated as 80% of the mean RT from the calibration block). During the test block, a go-response RT was considered as correct if it was below the 80% RT threshold of the immediately preceding calibration phase (FH). Otherwise, a feedback screen indicating "too late!" was displayed immediately after the go-response (SH). The instructions emphasized the speed of response over accuracy. SHs and FA were considered as errors in the calculation of the global feedback on performance displayed continuously on the top of the screen, such that the participants were also aware when they responded correctly. The global feedback indexing mean performance consisted of the cumulated accuracy expressed in percent correct. The index of mean performance was updated during the intertrial interval, immediately after the feedback on response speed for SH trials. No visual feedback on response speed was displayed after FHs or FAs (i.e., a response to a no-go stimulus; see Vocat, Pourtois, & Vuilleumier, 2008, for a similar procedure).

Participants were not informed about this thresholding procedure. The whole go/no-go training session included 528 stimuli ([160 stimuli in the test block + 16 stimuli in the calibration block] × 3 sessions = 528 stimuli) and lasted for ca. 35 min. After the completion of each session, a rest period of 10 min was provided to participants.

EEG Acquisition and Preprocessing

Continuous EEG was acquired at 1024 Hz through a 128-channel Biosemi ActiveTwo system (Biosemi, Amsterdam, Netherlands) referenced to the CMS-DRL ground (which functions as a feedback loop driving the average potential across the montage as close as possible to the amplifier zero). EEG data preprocessing and analyses were conducted using Cartool (sites.google.com/site/fbmlab/Cartool.htm; Brunet, Murray, & Michel, 2011). EEG epochs from 146 msec prestimulus to 146 msec poststimulus onset (i.e., 150 data points before and 150 data points after stimulus onset) were averaged, for each participant, for go and no-go trials following performance at preceding go stimuli, generating a 2 × 2 within-subject design with factors of "Preceding Performance" (SH, FH) and "Stimulus" (go vs. no-go; Figure 1). As we were interested in the processing of the stimulus as a function of previous performance, we locked the ERPs and focus our analyses to the stimulus and not to the response. Moreover, because processes occurring after 150 msec post-S2 onset were differentially contaminated by the initiation of the motor response as a function of factor stimulus (go but not no-go stimuli

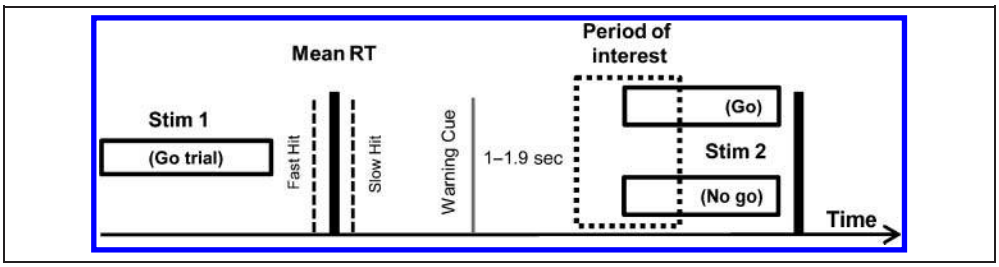

Figure 1. Experimental design. Each participant completed a 35-min go/no-go task. The period of interest comprises the processing of Stimulus 2 as a function a preceding performance (fast or slow).

were followed by a motor responses), we restricted our analyses with the initial 146 msec poststimulus onset period (mean RT was ca. 260 msec in our study [see Results section] and minimal latency of response initiation in the motor cortex occurs ca. 100 msec before the execution of the button press [Thorpe & Fabre-Thorpe, 2001]). We would note, however, that several lines of evidence report that response-related cortical motor activity already manifest 200–500 msec before response onset as, for example, the lateralized readiness potential, a measure of selective response preparation (Gratton, Coles, Siveraag, Ericksen, & Donchin, 1988; Kutas & Donchin, 1980). Although motor-related activity could have occurred during our period of interest, restraining our analyses to the first 150 msec lowered the probability of a contamination of our effects by motor responses. In addition, such contamination would have modulated the main effect of stimulus but not the main effect of preceding performance or the interaction term. In turn, this possible confound would not invalidate our results.

In addition to a ±80 μV artifact rejection criterion, EEG epochs containing eye blinks or other noise transients were removed after visual inspection. Before group averaging, data at artifact electrodes from each participant were interpolated using 3-D splines (Perrin, Bertrand, & Pernier, 1987). Data were band-pass filtered (0.18–40 Hz) and recalculated against the average reference. By removing slow drifts at the single epoch level, the low-pass filter resulted in a baseline correction on the whole epoch. Because one factor involved performance preceding stimulus onset, prestimulus differences could have been expected. Therefore, we did not apply a prestimulus baseline correction on our data.

The average number (±*SEM*) of accepted epochs was 57 ± 5.3 for the go preceded by an SH, 53.6 ± 5.5 for the go preceded by an FH, 62 ± 5.6 for the no-go preceded by an SH, and 53.3 ± 4.9 for the no-go preceded by an FH conditions. These values did not statistically differ ($p > .16$), ruling out that our effects followed from differences in signal-to-noise ratios across conditions.

Topographic Patterns Analyses

Topographic analyses were performed to determine whether the configuration of intracranial generators changed across either or both factors (i.e., preceding performance and stimulus type). These methods have been detailed elsewhere and have many analytical and interpretational benefits over canonical AEP waveform analyses (Tzovara, Murray, Michel, & De Lucia, in press; Murray, Brunet, & Michel, 2008). We provide only the essentials here. Major impetuses for the use of the present analyses were the ability to circumvent interpretational issues because of the reference-dependent nature of AEPs and to differentiate effects arising from topographic modulations from effects owing to changes in response strength. Moreover, the multivariate analyses used here require no selection either of the electrodes or periods of interest which are two major sources of potential bias in the statistical analysis of ERPs (Tzovara et al., in press). Still, we would be remiss to not acknowledge that a period of interest was defined by the experimenters during the act of epoching the continuous EEG into peristimulus intervals for signal averaging and ERP calculation. Likewise, parameters such as filtering and artifact rejection criteria were likewise selected by the experimenters.

The most dominant scalp topographies appearing in the AEPs of the group-averaged ERPs from each condition over time were identified with a *k*-means cluster analysis (Pascual-Marqui, Michel, & Lehmann, 1995). This approach is based on the observation that evoked potential topographies do not change randomly but rather remain for a period in a certain configuration and then switched to a new stable configuration (e.g., Murray et al., 2008; Michel et al., 2004). The optimal number of clusters to describe the data set is identified using a modified Krzanowski–Lai criterion (Tibshirani, Walther, Botstein, & Brown, 2005). These steps are all a hypothesis generation tool that is then statistically evaluated using single-subject data. Differences in the pattern of maps observed between conditions in the group-averaged data were tested by calculating the spatial correlation between these "template" maps from the group-averaged data and each time point of single-subject data from each experimental condition (referred to as "fitting"). For this fitting procedure, each time point of each AEP from each subject was labeled according to the map with which it best correlated spatially (see Murray et al., 2008; Brandeis, Lehmann, Michel, & Mingrone, 1995). The output of fitting is a measure of relative map presence in milliseconds, which indicates the amount of time over a given interval that each map that was identified in the group-averaged data best accounted for the response from a given individual subject and condition.

Electrical Source Estimations

We estimated the sources in the brain using a distributed linear inverse solution and the local autoregressive average (LAURA) regularization approach (Grave de Peralta, Gonzalez-Andino, & Gomez-Gonzalez, 2004; Grave de Peralta, Gonzalez-Andino, Lantz, Michel, & Landis, 2001; also Michel et al., 2004, for a comparison of inverse solution methods). LAURA selects the source configuration that better mimics the biophysical behavior of electric fields (i.e., activity at one point depends on the activity at neighboring points according to electromagnetic laws). Homogenous regression coefficients in all directions and within the whole solution space were used. For the lead field calculation, the Spherical Model with Anatomical Constrains method was applied (Spinelli, Andino, Lantz, Seeck, & Michel, 2000). This method first transforms the individual MRI to the best-fitting sphere using homogeneous transformation operators. It then determines a regular grid of 3005 solution points in the gray matter of this spherical MRI and computes the lead field matrix using the known analytical solution for a spherical head model with three shells of different conductivities as defined by Ary, Darcey, and Fender (1981).

To confirm and extend the above-described topographic analyses in the sensor space, we conducted a parallel analysis in the brain space independently to the topographic pattern analyses. Intracranial sources were estimated for each participant and condition and then statistically compared at each node level between conditions using the same within-subject design as in the topographic pattern analysis. Time-point wise 2 × 2 ANOVAs were computed with factors Preceding Performance and Stimulus for the 3005 solution points. A spatial criterion of a minimum of eight contiguous points and a duration criterion of 11 time samples was applied in the statistical parametric mapping procedure.

RESULTS

Behavioral Results

The performance with go stimuli was analyzed as a function of the performance on the preceding stimulus (S1), yielding two conditions for responses to go S2: those preceded by an SH or FH response to S1. We calculated PES effects as the number of SH following FH versus the number of SH following SH. Whether a given RT to go stimuli was considered as an SH or FH depended on its value relative to the RT threshold calculated during the RT calibration block that participants underwent before each test block. Because the threshold was determined for each participant individually and adjusted dynamically for each block of trials, we assume that the RT relative to individually determined response speed threshold is not the most sensitive index of response speed in our study. The mean absolute RTs for SH and FH occurrence for the four possible types of stimulus sequence (FH–FH, SH–FH, FH–SH, SH–SH) are displayed in Table 1. According to classical PES formula (difference between postcorrect trial RT and post-error trial RT), we report the differences in RT. RT for FH following FH or SH did not significantly differ ($t(9) = -0.63$, $p = .54$) nor did RT for SH following FH or SH differ ($t(9) = 0.59$, $p = .56$). However, as stated above, because of the individual calibration procedure implemented in our study and the separation of the RTs in FH and SH groups, the most relevant index of PES in our experimental paradigm is the relative number of FH and SH following accuracy at Stimulus 1.

The feedback "too late" was provided to the participants following SH. After an SH, participants committed more SH than FH ($t(9) = 4.16$; $p < .005$), replicating well-established PES effects (e.g., Ridderinkhof, Ullsperger, et al., 2004) and supporting that SH were indeed considered as error in our paradigm. After FHs, participants tended to commit more FH than SH, although not in a significant way ($t(9) = 1.66$; $p = .13$). These additional data are provided in Table 2.

The performance on no-go stimuli was analyzed as a function of the performance to the preceding stimuli. The percentage of FAs after an FH or after an SH did not statistically differ (6.39 ± 1.03% [7/109.4] and 6.75 ± 1.68% [8.5/125.9], respectively; $t(9) = -0.20$; $p = .84$). The absence of significant differences in FA as a function of the preceding performance likely followed from the fact that emphasis was put on speed over accuracy.

Electrical Neuroimaging Results

Topographic Pattern Analysis

K-means clustering was performed on the AEPs to identify the pattern of predominating topographies ("maps") of the electric field at the scalp in the cumulative group-averaged data. The output of the topographic pattern analysis is displayed in Figure 2A (see also exemplar AEP waveforms (C3 electrode)). The global explained variance of the results of the cluster analysis was 92.84%. This topographic pattern analysis identified the same sequence of stable maps for trials from the correct and error conditions and LG and RNG trial types with the exception of two

Table 1. Detailed Behavioral Effects of SH and FH Commission: RTs

Go1 Type–Go2 Type	*Go1 (msec)*	*Go2 (msec)*
FH–FH	213.4 ± 15.5	217.6 ± 16.6
FH–SH	211.6 ± 17.5	302.5 ± 27.9
SH–FH	316.6 ± 23.6	214.3 ± 19.2
SH–SH	301.6 ± 29.5	307.9 ± 32.5

Mean and *SEM* of RTs before and following SH or FH commission (in msec).

Table 2. Detailed Behavioral Effects of SH and FH Commission

Preceding Go Stimuli	*FH (n)*	*SH (n)*
FH	32.1 ± 4.5	24.7 ± 2.2
SH	17.1 ± 1.1	42.2 ± 5.5

Mean number and *SEM* of SHs or FHs as a function of previous performance.

periods. Over these periods, distinct sets of maps were observed first as a function of preceding performance and then as a function of the stimulus. The fitting procedure was then applied to the single-subject data from each condition to calculate the number of time points for each of the maps identified over the periods of topographic modulation observed in the group-averaged AEPs. This generated a quantification of how well each map accounted for an individual participant's AEPs over a given time interval. In the first time window (76–111 msec), there was a significant interaction between preceding performance and map ($F(1, 9) = 11.74$; $p < .01$; Figure 2B). In the second time window (113–146 msec), a significant interaction between stimulus and map was observed ($F(1, 9) = 4.84$; $p < .05$; Figure 2C). No other main effects or interactions were statistically reliable over either period.

Although several studies showed prestimulus differences as a function of accuracy (Pourtois, 2011; Hajcak, Nieuwenhuis, Ridderinkhof, & Simons, 2005), we did not take into account performance at the trial following FH or SH, representing a possible confound in the interpretation of our results. We did not sort trials as a function of performance because go and no-go stimuli were taken in account for the factor stimulus and that performance on these two trial types cannot not be assessed similarly (e.g., error to no-go trial are FA and error for go trials are too slow), the same rejection criterion based on performance cannot be applied to both trials type. Thus, the absence of effect during the prestimulus period could have resulted from a differential activity before successful versus unsuccessful trial that was not controlled in our study.

Source Estimations

A timeframe wise 2 × 2 ANOVA, with factors of Preceding Performance (SH, FH) and Stimulus (LG, RNG) was performed for each of the 3005 solution points. This analysis revealed a significant ($p < .05$) main effect of the Preceding Performance over the 104–126 msec period ($F(1, 9) > 5.12$; $p < .05$) and a main effect of Stimulus over the 122–146 msec interval ($F(1, 9) > 5.12$; $p < .05$), but no interaction between these factors at any point in time. These periods and the sequence of main effects corresponded to those observed in the above analyses of the surface-recorded AEPs. The slight differences between the period of the effects revealed by the topographic and sources analyses could follow from the fact that data were reduced in time by the clustering procedure applied during the temporal segmentation of the ERPs but not during the time-wise analyses of the inverse solutions (e.g., Murray et al., 2008). The topographic pattern analyses thereby relied on a reduced number of periods of stable

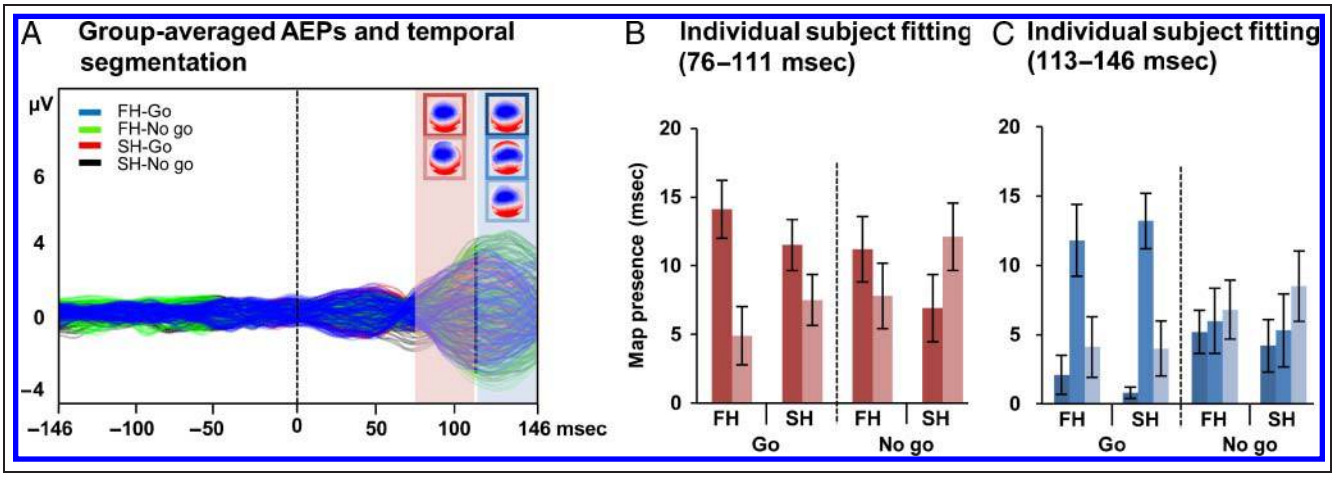

Figure 2. (A) The AEP in response to go (blue trace) and no-go (black) stimuli preceded by SHs and go (red) and no-go (green) preceded by FHs are displayed in microvolts as a function of time. Topographic pattern analyses in the group-averaged AEPs identified two periods of stable electric field topography where multiple maps were differentially engaged as a function of the experimental conditions: 76–111 msec (framed in red) and 113–146 msec (framed in blue). All topographies (i.e., maps) are shown with the nasion upward and left scalp leftward. The reliability of this observation at the group-averaged level was then assessed at the single-subject level using a spatial correlation fitting procedure (see Methods). (B) Over the 76–111 msec poststimulus period, different maps (framed in dark and light red) described AEPs in response to stimulus (go/no-go) as a function of preceding performance (FH/SH). There was a significant main effect of Preceding Performance. Error bars indicate *SEM*. (C) Over the 113–146 msec poststimulus period, different maps again (framed in dark and light blue) described AEPs in response to stimulus (go/no-go) as a function of preceding performance (FH/SH). Results showed a significant main effect of factor Stimulus. Error bars indicate *SEM*.

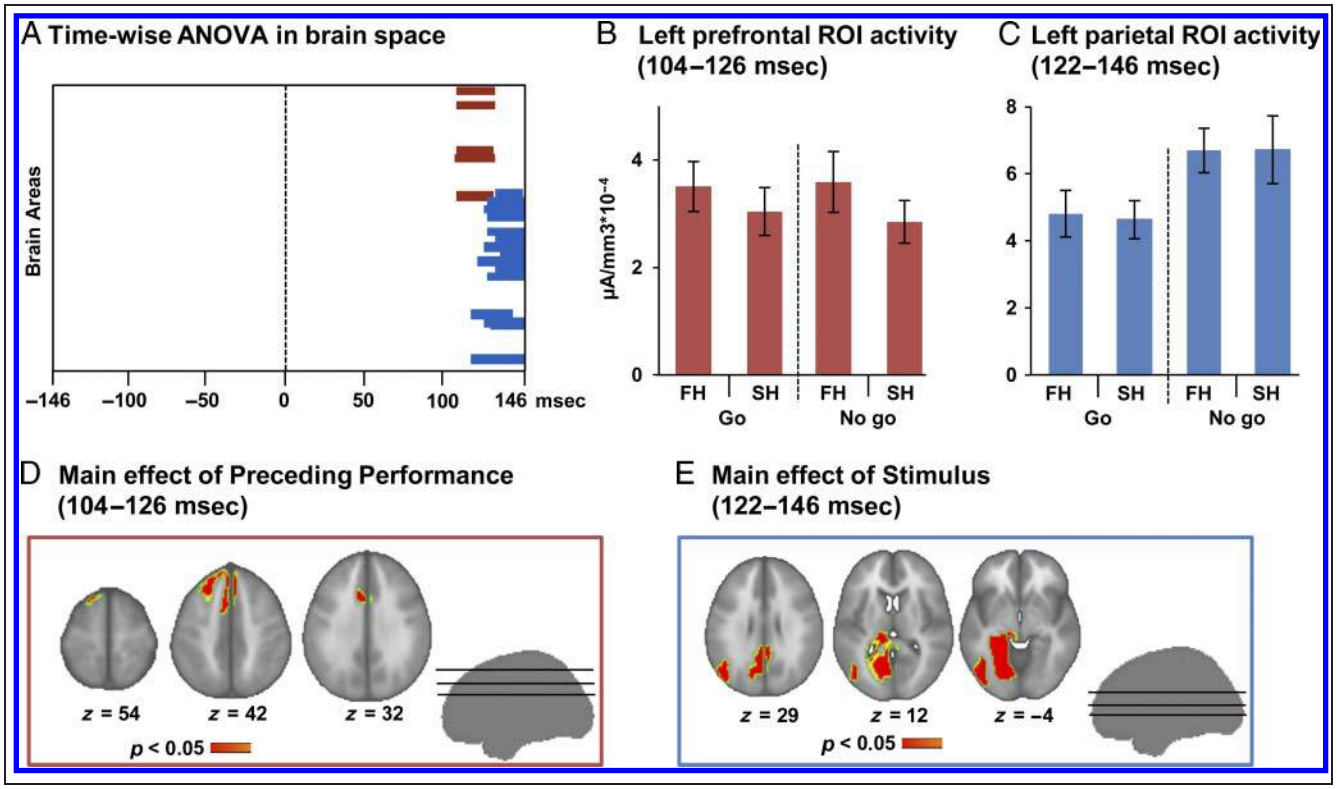

Figure 3. (A) Time-wise ANOVA in brain space is displayed as a function of time. The *y* axis shows the brain space merged in 80 ROIs (AAL space), organized from frontal (top) to occipital (bottom) brains areas. Red bars indicate significant main effect of Preceding Performance. Blue bars represent a significant main effect of Stimulus. (B) Follow-up analyses on the mean scalar value of the prefrontal ROI revealed a decrease in left pFCs following an SH relative to an FH. (C) Follow-up analyses on the mean scalar value of the parietal ROI revealed a decrease in left parietal cortices for the processing of go stimulus relative to no-go. (D) The main effect of preceding performance included a prefrontal cluster comprising the ACC and the DLPFC. (E) The main effect of stimuli included a parietal cluster comprising the precuneus, the posterior cingulate cortex, the parahippocampal gyrus, the fusiform gyrus, the lingual gyrus, the middle and inferior occipital gyri, the middle temporal gyrus, and the angular gyrus. Brain slices are displayed in *z*-coordinates in the MNI space.

microstate as compared with the source analyses, which was performed at each time frame. Figure 3A displays LAURA distributed source estimations averaged over the post-stimulus period when the timeframe wise ANOVA showed significant main effects of factor Preceding Performance and factor Stimulus. To facilitate the visualization of the temporal dynamics of the effects in Figure 3A, we down-sampled the 3005 solution points into the 80 ROIs of the AAL space (Tzourio-Mazoyer et al., 2002). The AAL ROIs are arranged from anterior (up) to posterior (down) regions along the *y* axis. The brain regions showing the main effect of factor Preceding Performance comprised ACC and DLPFC (Figure 3D) and the main effect of Stimuli at the left parietal cluster comprising the precuneus, the posterior cingulate cortex, the parahippocampal gyrus, the fusiform gyrus, the lingual gyrus, the middle and inferior occipital gyri, the middle temporal gyrus, and the angular gyrus (Figure 3E).

To determine the direction of these effects, AEPs for each participant and each experimental condition separately were first averaged across the period of interest to generate one data point per participant and experimental condition. Source estimations were then calculated, and the scalar value of each solution point comprised within the ROI, showing the main effect of Preceding Performance as well as Stimulus, were extracted and averaged separately for each subject and condition. The main effect of Preceding Performance followed from a significant decrease in the activation strength of the left prefrontal ROI for SH as compared with FH followed either by a go or no-go stimulus type (Figure 3B). The main effect of Stimulus followed from a lower activation of the left parietal ROI for go than no-go stimuli in both FH and SH conditions (Figure 3C).

To determine whether and how the prefrontal and parietal ROIs were functionally coupled, we performed a correlational analysis. The correlations were performed between factor Preceding Performance (FH or SH) and factor Stimulus irrespective of stimulus type, that is, activity of the parietal ROI were averaged between the go and no-go condition before the calculation of the correlations. This analysis revealed a significant correlation between prefrontal cluster and parietal clusters when the preceding performance was FH ($r(8) = 0.72$, $p < .02$). There was only a nonsignificant tendency for such a correlation in the SH condition ($r(8) = 0.58$, $p = .07$). The activity of prefrontal and parietal clusters is functionally coupled after FH, but not after the participant made an SH.

Correlational analysis showed significant negative correlations between the parietal ROIs activity and log-transformed RT both at FH and SH ($r(8) = -0.67, p < .05$; $r(8) = -0.65$, $p < .05$, respectively). These results indicate that the more the parietal ROI was active after an FH or an SH, the more the participants slowed down their responses.

DISCUSSION

Behaviorally, we replicated previous evidence for PES effects (e.g., Li et al., 2008). As compared with FH, SHs, considered as errors in our paradigm, induced a significant increase in the number of SH. We contrasted electrical neuroimaging responses to go and no-go stimuli as a function of the performance to the preceding stimuli. Our results showed that AEPs modulated topographically as a function of whether participants made an error or not on the preceding trial 70–110 msec post-onset, indicative of the engagement of distinct configurations of intracranial generators. Then AEP modulated topographically as a function of stimulus type 110–150 msec. A second level of time-wise statistical analyses conducted in the brain space independently to the topographic pattern analyses revealed an identical sequence of effects. Source estimations revealed a significantly stronger activity within prefrontal regions to go and no-go stimuli following FH than SH trials over the 100–120 msec poststimulus onset. This effect was followed by a stronger response of parietal areas to the no-go than go stimulus type 120–140 msec independently of preceding performance. This pattern of results suggests that errors in a speeded go/no-go task modulate early, low-level integration of the following stimuli, in turn influencing subsequent inhibitory proficiency. By capitalizing on prior but not current performance to contrast brain activity to trial processed with low versus high inhibitory proficiency, we were able to assess the effect of factor "stimulus type" in our design, that is, including no-go trials for which no behavioral responses were measured. This approach allowed to assess the effect of inhibitory proficiency in conditions where responses had to be elicited or not.

As go/no-go performance on a given trial determines inhibitory proficiency at the subsequent trial (i.e., response speed decrease following errors; Lawrence, Luty, Bogdan, Sahakian, & Clark, 2009; Rabbit, 1966), by contrasting AEPs to the auditory stimuli as a function of the preceding performance, we actually contrasted brain responses to the stimuli in a situation in which efficient versus inefficient inhibitory control processes were engaged. Accordingly, we hypothesize that the main effect of preceding performance at 120 msec poststimulus onset reflects distinct response modes, allowing either fast or slow inhibitory control.

Recent models of inhibitory control suggest that optimal go/no-go performance is achieved by adopting an automatic form of inhibition, involving a feedforward control of stimulus–response mapping by parieto-prefrontal executive networks over the very initial stages of sensory integration (Manuel et al., 2010; Verbruggen & Logan, 2008; Logan, 1988; Shiffrin & Schneider, 1977). An automatic response mode would allow for increasing the speed of go/no-go decisions by shortcutting inputs from slow, controlled top–down executive modules (Kenner et al., 2010; Manuel et al., 2010). We would note that the term "automaticity" as used here not only refers to automatic responses to go stimuli because of the response prepotency induced by task instruction but also to the fact that no-go goals consisting in inhibiting motor response are no more solely supported by controlled processes once stimulus–response mapping rules are learned. Because the stimulus–response mapping rule was straightforward in our study and that emphasis was put on speed rather than on accuracy (negative feedback was provided after two SHs, and the later trials were counted as errors), participants were likely engaged in such automatic response mode during most of the trials. Further supporting that participants actually responded on the basis of speed rather than accuracy, response speed but not accuracy was modulated by practicing the go/no-go task in this study (Manuel et al., 2010). RTs for FH corresponded to the minimal physiological response speed in such tasks (Manuel et al., 2010) corresponding to asymptotic RT of approximately 200 msec.

However, the detection of errors would have broken down the engagement of automatic inhibition and increased the level of top–down executive control, in turn slowing down responses.

Supporting this hypothesis, we showed that the effect of preceding performance manifesting as topographic modulation over the 100–120 msec poststimulus onset followed from lower activity within prefrontal regions after SH than FH. This finding fits well with traditional views holding that error detection modulates dorsomedial pFCs comprising top–down executive mechanisms involved in subsequent behavioral adjustment (e.g., Li et al., 2008; Kerns et al., 2004; Ridderinkhof, van den Wildenberg, et al., 2004; Botvinick et al., 2001). For instance, Kerns et al. (2004) showed that the greater pFC was activated following errors, the greater were PES effects. In addition, animal data indicate that DLPFC activity reflects conflict level and maintain information about previous conflict in memory (Mansouri, Buckley, & Tanaka, 2007).

However, the direction of our effect contrasts with previous evidence for an increased prefrontal activity accompanying the engagement of top–down executive control following error detection (Kerns et al., 2004; Garavan et al., 2002). This apparent discrepancy might follow from differences in the period of interest examined in these studies. Our effect manifested during the processing of the subsequent stimuli and not immediately after the detection of the error, as investigated in previous literature (Ullsperger & von Cramon, 2001; Falkenstein et al., 2000). Supporting this explanation, differential activation patterns of pFC during error detection and subsequent processing have indeed been shown when these

phases were analyzed as separate within-trial processes. For instance, Chevrier and Schachar (2010) showed deactivation of medial pFC during error detection but increased activity in the same regions during subsequent PES. Activity within these structures was also found to decrease during cognitive tasks requiring mental effort or goal-directed behaviors (Tomasi, Ernst, Caparelli, & Chang, 2006; Greicius & Menon, 2004; Raichle et al., 2001). Alternatively, medial versus lateral pFCs have been shown to dynamically adjust their relative activity, depending on task demand, which could explain discrepancies between activation versus deactivation patterns of these areas between previous literature and our results. Medial pFC consistently shows increased activity during rest or low-demand across a wide range of tasks, compared with high demanding tasks (Mazoyer et al., 2001; Shulman et al., 1997; see also Hester & Garavan, 2004, for a deactivation in the left medial frontal gyrus before stopping in a response inhibition task). This default mode network is typically inversely correlated with lateral prefrontal regions, suggesting there to be a "dynamic equilibrium" between medial and lateral prefrontal regions (Greicius, Krasnow, Reiss, & Menon, 2003). The engagement in complex cognitive processes would be supported by a reallocation of neural resources from default mode medial areas to lateral prefrontal regions (Greicius & Menon, 2004).

The issue of a hemispheric specialization of the brain mechanisms supporting inhibitory processes and post-error behavioral adjustment remain debated. Kerns et al. (2004) reported post-error behavioral adjustments to be associated with activity in the right DLPFC. Further evidence also pointed the right DLPFC might contribute to on-line behavioral adjustments by amplifying task-relevant features (King, Korb, von Cramon, & Ullsperger, 2010; Egner & Hirsch, 2005). By contrast, several studies document a role for the left pFC in behavioral adjustment (Garavan et al., 2002; Kiehl, Liddle, & Hopfinger, 2000) and suggest that the left DLPFC would support maintenance of task sets (MacDonald et al., 2000). Garavan et al. (2002) further proposed the left pFC to be mostly activated by tonic inhibitory tasks in which inhibition processes must be sustained over a period rather than phasic inhibitory tasks such as the go/no-go task. Although top–down attentional processes are commonly associated to the left DLPFC (MacDonald et al., 2000), recent research revealed an essential role of the right DLPFC in task preparation (Vanderhasselt, De Raedt, Baeken, Leyman, & D'haenen, 2006; Brass & von Cramon, 2004). A recent review by Vanderhasselt, De Raedt, and Baeken (2009), suggest that the left DLPFC is activated when attentional adjustments are required regarding the processing of upcoming stimulus. Whereas the left DLPFC does not seem to be activated in the presence of conflict in the Stroop task, the right DLPFC is activated in conflict-driven cognitive control. Finally, basic task parameters could also participate in the lateralization of the effects related to behavioral adjustment and inhibitory control. For instance, in our task, the left lateralization of the main effect of Preceding Performance might also follow from the fact that participants responded with their right hand, which could have required the engagement inhibitory processes comprised within the same hemisphere as the motor areas solicited during the task.

That pFCs modulated at a latency of 100–120 msec poststimulus onset as a function of inhibitory proficiency further supports that it may reflect the differential involvement of early-stage forms of inhibition. Previous ERP studies of go/no-go tasks indeed demonstrate that the suppression of prepotent responses by top–down executive modules manifests over processing stages subsequent to initial sensory encoding, around 150–400 msec (Kaiser et al., 2006; Falkenstein et al., 1999; Kiefer, Marzinzik, Weisbrod, Scherg, & Spitzer, 1998).

According to recent hypotheses on the mechanisms mediating PES, the switch between automatic to top–down executive control could have been caused by an attentional modulation. PES has been advanced to follow from the need to refocus attention to the task following distraction induced by the infrequent error trials (orienting hypothesis: Nunez Castellar et al., 2010; Notebaert et al., 2009; Taylor et al., 2007) or error-related increase in arousal (Carp & Compton, 2009). Similarly, King et al. (2010) reported that PES could be because of the interference of the OR with task preparation and stimulus processing. Arguing against this hypothesis, we did not find evidence for modulation in attention-related areas during the prestimulus period (Brass, Derrfuss, Forstmann, & von Cramon, 2005). However, the prestimulus period analyses here were perhaps too short, which prevented to reveal the role of attention in the switch between the automatic versus controlled response mode. In addition, our analyses would not have caught nonphase locked attention-related processes manifesting at the level of oscillatory activity. Previous evidence indeed suggest that modulations in attention, supporting, for example, the anticipation of forthcoming stimuli manifest as an increase in the power of oscillation in the alpha frequency band in the hemisphere contralateral to the attended hemispace (Rihs, Michel, & Thut, 2009; Romei et al., 2008; Thut, Nietzel, Brandt, & Pascual-Leone, 2006). Because go stimuli were always presented in the left hemispace, the participants possibly learned to attend to the left for increasing response speed, yielding a main effect of stimuli during the prestimulus period in oscillatory activity.

Errors constitute a strong negative reinforcement learning signal; in this regard, the effect of error in the processing of subsequent stimuli is interpretable in terms of reflecting changes in associative learning. Interestingly, recent evidence shows that modifications in learned stimulus–response mapping associations depend on error-related activity within medial pFCs when feedback is provided to participants (Hester et al., 2010). This finding indicates that processes related to monitoring and reweighting of

a behavior's value parallel those related to increases in executive control within prefrontal areas following errors; both mechanisms impacting how subsequent stimuli are handled. Because they shape stimulus–response mapping rules, feedback-related learning mechanisms likely participate to plastic brain mechanisms underlying the development of automatic feedforward forms of inhibitory processes developing with go/no-go training as observed in Manuel et al. (2010; see also Verbruggen & Logan, 2008).

Go and no-go stimuli were differentially processed within parietal structures in the period immediately following the main effect of factor Preceding Performance, 120–140 msec poststimulus onset. Importantly, the activity within this parietal cluster positively correlated with the prefrontal clusters following FH but not SHs. We interpret this finding in terms of a facilitation of stimulus–response mapping processes occurring within parietal areas by prefrontal areas supporting fast inhibitory control. The stimulus–response mapping would directly depend on prefrontal areas during automatic response mode, but not in the top–down executive control engaged following errors.

Fronto-parietal circuits have been repeatedly implicated in action planning and initiation, with the degree of interaction between these areas modulating as a function of participants' control over responses (e.g., Pesaran, Nelson, & Andersen, 2008). These reports are in line with our hypothesis for a role of attention in switching between automatic to top–down response modes following errors. When no errors are committed, automatic control of response inhibition would be engaged and supported by a functional coupling between prefrontal and parietal areas. Following errors, however, top–down control would be engaged and this functional interaction would break down. Consistently, Prado, Carp, and Weissman (2010) linked reduced functional connectivity between the prefrontal and parietal cortices with increases in RT during a selective attention task, suggesting that, mediated by attention, the communication between these regions would facilitate response selection (Rushworth, Buckley, Behrens, Walton, & Bannerman, 2007) and action planning (Andersen & Cui, 2009).

Medial parietal regions, notably the precuneus, play a critical role in shifting attention toward relevant stimulus–response associations (Corbetta & Shulman, 2002; Rushworth, Paus, & Sipila, 2001). Moreover, stimulus–response mapping repertoires have been advanced to preactivate within parietal cortices (Barber & Carter, 2005; Ridderinkhof, van den Wildenberg, et al., 2004). Accordingly, during the prestimulus anticipatory period, parietal structures would send signals for increasing alertness and preactivating relevant stimulus–response associations (Barber & Carter, 2005; Astafiev et al., 2003; Rushworth et al., 2001).

Parietal structures are a suitable candidate for comprising stimulus–response mapping mechanisms involved in initiating or inhibiting motor responses based on the spatial attributes of the auditory go and no-go stimuli. Relative to the mean RT in our study, the 120–140 msec interval when main effect of stimulus type manifested corresponds to the period of motor response initiation (at ca. 130 msec post S2 onset, 130 msec before the mean RT (Thorpe & Fabre-Thorpe, 2001). On one hand, parietal structures have been involved in the interfacing between sensory signals and motor command (Andersen, Snyder, Bradley, & Xing, 1997), in the response preparation processes including control of motor planning (Ruge et al., 2005; Brass & von Cramon, 2004) or preparation for movements (Deiber, Ibanez, Sadato, & Hallett, 1996). Supporting these results, we recently demonstrated that parietal areas support learned associations between stimuli and behavioral responses early in the processing of a stimulus in a go/no-go task (Manuel et al., 2010). On the other hand, parietal structures are also involved in discriminating the spatial attributes of the stimuli (Spierer, Murray, Tardif, & Clarke, 2008; Spierer, Tardif, Sperdin, Murray, & Clarke, 2007). Accordingly, we would note that in our study go stimuli were always presented on the left and no-go on the right hemispace. These acoustic differences, coupled with the well-established functional lateralization of auditory spatial processing, could have biased the main effect of stimuli and thus limit the related interpretations. Furthermore, we cannot rule out from our data that participant paid more attention to the left hemispace from where go stimuli came and therefore that the main effect of stimuli reflected differential attention to go and no-go stimuli in addition to their acoustic difference. Further investigations, involving control of acoustic differences between go and no-go stimuli by, for example, reversing the SR mapping rule in half of the experiment would be necessary to disentangle this issue.

Collectively, our results support a model of executive control wherein either feedforward/automatic or top–down/controlled forms of inhibition can be engaged to resolve go/no-go tasks. In the former, stimulus response mapping is directly dependent on the activity of prefrontal executive module activated over the initial stage of cortical integration of the stimuli, allowing for fast response inhibition to no-go stimuli and in turn, fast RT to go stimuli. More consciously controlled top–down form of inhibition would instead involve higher-order executive modules activated by attention following error or in situation of new or complex stimulus–response mapping rules (Verbruggen & Logan, 2008). According to this model, PES would reflect a switch from automatic to controlled form of inhibition induced by errors.

Acknowledgments

This work was supported by a grant from the Pierre Mercier Foundation for Science to L. S.; M. M. M. was supported by the Swiss National Science Foundation (Grant 310030B-133136). The Cartool software (sites.google.com/site/fbmlab/Cartool.htm) has been programmed by Denis Brunet, from the Functional Brain Mapping Laboratory, Geneva, Switzerland, and was supported by the Center for Biomedical Imaging of Geneva and Lausanne. We thank Gilles Pourtois and Roland Vocat for their help in programming the experimental design.

Reprint requests should be sent to Aurelie L. Manuel, Faculty of Biology and Medicine (UNIL), Neuropsychology and Neurorehabilitation Service (CHUV), av. Pierre-Decker 5 1011, Lausanne, Switzerland, or via e-mail: aurelie.manuel@chuv.ch.

REFERENCES

Andersen, R. A., & Cui, H. (2009). Intention, action planning, and decision making in parietal-frontal circuits. *Neuron, 63,* 568–583.

Andersen, R. A., Snyder, L. H., Bradley, D. C., & Xing, J. (1997). Multimodal representation of space in the posterior parietal cortex and its use in planning movements. *Annual Review of Neuroscience, 20,* 303–330.

Ary, J. P., Darcey, T. M., & Fender, D. H. (1981). A method for locating scalp electrodes in spherical coordinates. *IEEE Transactions on Biomedical Engineering, 28,* 834–836.

Astafiev, S. V., Shulman, G. L., Stanley, C. M., Snyder, A. Z., Van Essen, D. C., & Corbetta, M. (2003). Functional organization of human intraparietal and frontal cortex for attending, looking, and pointing. *Journal of Neuroscience, 23,* 4689–4699.

Barber, A. D., & Carter, C. S. (2005). Cognitive control involved in overcoming prepotent response tendencies and switching between tasks. *Cerebral Cortex, 15,* 899–912.

Blauert, J. (1997). *Spatial hearing* (revised edition). Cambridge, MA: MIT Press.

Botvinick, M. M., Braver, T. S., Barch, D. M., Carter, C. S., & Cohen, J. D. (2001). Conflict monitoring and cognitive control. *Psychological Review, 108,* 624–652.

Brandeis, D., Lehmann, D., Michel, C. M., & Mingrone, W. (1995). Mapping event-related brain potential microstates to sentence endings. *Brain Topography, 8,* 145–159.

Brass, M., Derrfuss, J., Forstmann, B., & von Cramon, D. Y. (2005). The role of the inferior frontal junction area in cognitive control. *Trends in Cognitive Sciences, 9,* 314–316.

Brass, M., & von Cramon, D. Y. (2004). Selection for cognitive control: A functional magnetic resonance imaging study on the selection of task-relevant information. *Journal of Neuroscience, 24,* 8847–8852.

Brown, J. W., & Braver, T. S. (2005). Learned predictions of error likelihood in the anterior cingulate cortex. *Science, 18,* 1118–1121.

Brunet, D., Murray, M. M., & Michel, C. M. (2011). Spatio-temporal analysis of multichannel EEG: CARTOOL. *Computational Intelligence and Neuroscience, 2011,* 813870.

Carp, J., & Compton, R. J. (2009). Alpha power is influenced by performance errors. *Psychophysiology, 46,* 336–343.

Carter, C. S., & van Veen, V (2007). Anterior cingulate cortex and conflict detection: An update of theory and data. *Cognitive, Affective & Behavioral Neuroscience, 7,* 367–379.

Chevrier, A., & Schachar, R. J. (2010). Error detection in the stop signal task. *Neuroimage, 53,* 664–673.

Corbetta, M., & Shulman, G. L. (2002). Control of goal-directed and stimulus-driven attention in the brain. *Nature Reviews Neuroscience, 3,* 201–215.

Deiber, M. P., Ibanez, V., Sadato, N., & Hallett, M. (1996). Cerebral structures participating in motor preparation in humans: A positron emission tomography study. *Journal of Neurophysiology, 75,* 233–247.

Dikman, Z. V., & Allen, J. J. (2000). Error monitoring during reward and avoidance learning in high- and low-socialized individuals. *Psychophysiology, 37,* 43–54.

Dimoska, A., Johnstone, S. J., & Barry, R. J. (2006). The auditory-evoked N2 and P3 components in the stop-signal task: Indices of inhibition, response-conflict or error detection? *Brain and Cognition, 62,* 98–112.

Egner, T., & Hirsch, J. (2005). The neural correlates and functional integration of cognitive control in a Stroop task. *Neuroimage, 24,* 539–547.

Falkenstein, M., Hoormann, J., Christ, S., & Hohnsbein, J. (2000). ERP components on reaction errors and their functional significance: A tutorial. *Biological Psychology, 51,* 87–107.

Falkenstein, M., Hoormann, J., & Hohnsbein, J. (1999). ERP components in go/no-go tasks and their relation to inhibition. *Acta Psychologica (Amsterdam), 101,* 267–291.

Falkenstein, M., Koshlykova, N. A., Kiroj, V. N., Hoormann, J., & Hohnsbein, J. (1995). Late ERP components in visual and auditory Go/Nogo tasks. *Electroencephalography Clinical Neurophysiology, 96,* 36–43.

Fiehler, K., Ullsperger, M., & von Cramon, D. Y. (2004). Neural correlates of error detection and error correction: Is there a common neuroanatomical substrate? *European Journal of Neuroscience, 19,* 3081–3087.

Frank, M. J., Seeberger, L. C., & O'Reilly, R. C. (2004). By Carrot or by stick: Cognitive reinforcement learning in parkinsonism. *Science, 306,* 1940–1943.

Frank, M. J., Woroch, B. S., & Curran, T. (2005). Error-related negativity predicts reinforcement learning and conflict biases. *Neuron, 47,* 495–501.

Garavan, H., Ross, T. J., Murphy, K., Roche, R. A., & Stein, E. A. (2002). Dissociable executive functions in the dynamic control of behavior: Inhibition, error detection, and correction. *Neuroimage, 17,* 1820–1829.

Gehring, W. J., Goss, B., Coles, M. G. H., Meyer, D. E., & Donchin, E. (1993). A neural system for error detection and compensation. *Psychological Science, 4,* 385–390.

Gratton, G., Coles, M. G., Siveraag, E. J., Ericksen, C. W., & Donchin, E. (1988). Pre- and poststimulus activation of response channels: A psychophysiological analysis. *Journal of Experimental Psychology: Human Perception and Performance, 14,* 331–344.

Grave de Peralta, R., Gonzalez-Andino, S., & Gomez-Gonzalez, C. M. (2004). The biophysical foundations of the localisation of encephalogram generators in the brain. The application of a distribution-type model to the localisation of epileptic foci. *Revista de Neurologia, 39,* 748–756.

Grave de Peralta, R., Gonzalez-Andino, S., Lantz, G., Michel, C. M., & Landis, T. (2001). Noninvasive localization of electromagnetic epileptic activity. I. Method descriptions and simulations. *Brain Topography, 14,* 131–137.

Greicius, M. D., Krasnow, B., Reiss, A. L., & Menon, V. (2003). Functional connectivity in the resting brain: A network analysis of the default mode hypothesis. *Proceedings of the National Academy of Sciences, U.S.A., 100,* 253–258.

Greicius, M. D., & Menon, V. (2004). Default-mode activity during a passive sensory task: Uncoupled from deactivation but impacting activation. *Journal of Cognitive Neuroscience, 16,* 1484–1492.

Hajcak, G., Nieuwenhuis, S., Ridderinkhof, K. R., & Simons, R. F. (2005). Error-preceding brain activity: Robustness, temporal dynamics, and boundary conditions. *Biological Psychology, 70,* 67–78.

Hester, R., Barre, N., Murphy, K., Silk, T. J., & Mattingley, J. B. (2008). Human medial frontal cortex activity predicts learning from errors. *Cerebral Cortex, 18,* 1933–1940.

Hester, R., & Garavan, H. (2004). Executive dysfunction in cocaine addiction: Evidence for discordant frontal, cingulate, and cerebellar activity. *Journal of Neuroscience, 24,* 11017–11022.

Hester, R., Murphy, K., Brown, F. L., & Skilleter, A. J. (2010). Punishing an error improves learning: The influence of punishment magnitude on error-related neural activity and subsequent learning. *Journal of Neuroscience, 30,* 15600–15607.

Hester, R., Simoes-Franklin, C., & Garavan, H. (2007). Post-error behavior in active cocaine users: Poor awareness of errors in the presence of intact performance adjustments. *Neuropsychopharmacology, 32,* 1974–1984.

Holroyd, C. B., & Coles, M. G. (2002). The neural basis of human error processing: Reinforcement learning, dopamine, and the error-related negativity. *Psychological Review, 109,* 679–709.

Holroyd, C. B., Yeung, N., Coles, M. G., & Cohen, J. D. (2005). A mechanism for error detection in speeded response time tasks. *Journal of Experimental Psychology: General, 134,* 163–191.

Kaiser, S., Weiss, O., Hill, H., Markela-Lerenc, J., Kiefer, M., & Weisbrod, M. (2006). N2 event-related potential correlates of response inhibition in an auditory go/no-go task. *International Journal of Psychophysiology, 61,* 279–282.

Kenner, N. M., Mumford, J. A., Hommer, R. E., Skup, M., Leibenluft, E., & Poldrack, R. A. (2010). Inhibitory motor control in response stopping and response switching. *Journal of Neuroscience, 30,* 8512–8518.

Kerns, J. G., Cohen, J. D., MacDonald, A. W., III, Cho, R. Y., Stenger, V. A., & Carter, C. S. (2004). Anterior cingulate conflict monitoring and adjustments in control. *Science, 303,* 1023–1026.

Kiefer, M., Marzinzik, F., Weisbrod, M., Scherg, M., & Spitzer, M. (1998). The time course of brain activations during response inhibition: Evidence from event-related potentials in a go/no-go task. *NeuroReport, 9,* 765–770.

Kiehl, K. A., Liddle, P. F., & Hopfinger, J. B. (2000). Error processing and the rostral anterior cingulate: An event-related fMRI study. *Psychophysiology, 37,* 216–223.

King, J. A., Korb, F. M., von Cramon, D. Y., & Ullsperger, M. (2010). Post-error behavioral adjustments are facilitated by activation and suppression of task-relevant and task-irrelevant information processing. *Journal of Neuroscience, 30,* 12759–12769.

Kutas, M., & Donchin, E. (1980). Preparation to respond as manifested by movement-related brain potentials. *Brain Research, 202,* 95–115.

Lawrence, A. J., Luty, J., Bogdan, N. A., Sahakian, B. J., & Clark, L. (2009). Impulsivity and response inhibition in alcohol dependence and problem gambling. *Psychopharmacology (Berlin), 207,* 163–172.

Li, C. S., Huang, C., Yan, P., Paliwal, P., Constable, R. T., & Sinha, R. (2008). Neural correlates of post-error slowing during a stop signal task: A functional magnetic resonance imaging study. *Journal of Cognitive Neuroscience, 20,* 1021–1029.

Logan, G. D. (1988). Automaticity, resources, and memory: Theoretical controversies and practical implications. *Human Factors, 30,* 583–598.

MacDonald, A. W., III, Cohen, J. D., Stenger, V. A., & Carter, C. S. (2000). Dissociating the role of the dorsolateral prefrontal and anterior cingulate cortex in cognitive control. *Science, 288,* 1835–1838.

Mansouri, F. A., Buckley, M. J., & Tanaka, K. (2007). Mnemonic function of the dorsolateral prefrontal cortex in conflict-induced behavioral adjustment. *Science, 318,* 987–990.

Manuel, A. L., Grivel, J., Bernasconi, F., Murray, M. M., & Spierer, L. (2010). Brain dynamics underlying training-induced improvement in suppressing inappropriate action. *Journal of Neuroscience, 30,* 13670–13678.

Mazoyer, B., Zago, L., Mellet, E., Bricogne, S., Etard, O., Houdé, O., et al. (2001). Cortical networks for working memory and executive functions sustain the conscious resting state in man. *Brain Research Bulletin, 54,* 287–298.

Michel, C. M., Murray, M. M., Lantz, G., Gonzalez, S., Spinelli, L., & Grave de Peralta, R. (2004). EEG source imaging. *Clinical Neurophysiology, 115,* 2195–2222.

Murray, M. M., Brunet, D., & Michel, C. M. (2008). Topographic ERP analyses: A step-by-step tutorial review. *Brain Topography, 20,* 249–264.

Nieuwenhuis, S., Holroyd, C. B., Mol, N., & Coles, M. G. (2004). Reinforcement-related brain potentials from medial frontal cortex: Origins and functional significance. *Neuroscience Biobehavioral Reviews, 28,* 441–448.

Notebaert, W., Houtman, F., Opstal, F. V., Gevers, W., Fias, W., & Verguts, T. (2009). Post-error slowing: An orienting account. *Cognition, 111,* 275–279.

Nunez Castellar, E., Kuhn, S., Fias, W., & Notebaert, W. (2010). Outcome expectancy and not accuracy determines posterror slowing: ERP support. *Cognitive, Affective & Behavioral Neuroscience, 10,* 270–278.

Oldfield, R. C. (1971). The assessment and analysis of handedness: The Edinburgh inventory. *Neuropsychologia, 9,* 97–113.

Pascual-Marqui, R. D., Michel, C. M., & Lehmann, D. (1995). Segmentation of brain electrical activity into microstates: Model estimation and validation. *IEEE Transactions on Biomedical Engineering, 42,* 658–665.

Perrin, F., Bertrand, O., & Pernier, J. (1987). Scalp current density mapping: Value and estimation from potential data. *IEEE Transactions on Biomedical Engineering, 34,* 283–288.

Pesaran, B., Nelson, M. J., & Andersen, R. A. (2008). Free choice activates a decision circuit between frontal and parietal cortex. *Nature, 453,* 406–409.

Pourtois, G. (2011). Early error detection predicted by reduced pre-response control process: An ERP topographic mapping study. *Brain Topography, 23,* 403–422.

Prado, J., Carp, J., & Weissman, D. H. (2010). Variations of response time in a selective attention task are linked to variations of functional connectivity in the attentional network. *Neuroimage, 54,* 541–549.

Rabbit, P. M. A. (1966). Errors and error correction in choice-response tasks. *Journal of Experimental Psychology, 71,* 264–272.

Raichle, M. E., MacLeod, A. M., Snyder, A. Z., Powers, W. J., Gusnard, D. A., & Shulman, G. L. (2001). A default mode of brain function. *Proceedings of the National Academy of Sciences, U.S.A., 98,* 676–682.

Ridderinkhof, K. R., Ullsperger, M., Crone, E. A., & Nieuwenhuis, S. (2004). The role of the medial frontal cortex in cognitive control. *Science, 306,* 443–447.

Ridderinkhof, K. R., van den Wildenberg, W. P., Segalowitz, S. J., & Carter, C. S. (2004). Neurocognitive mechanisms of cognitive control: The role of prefrontal cortex in action selection, response inhibition, performance monitoring, and reward-based learning. *Brain and Cognition, 56,* 129–140.

Rihs, T. A., Michel, C. M., & Thut, G. (2009). A bias for posterior alpha-band power suppression versus enhancement during shifting versus maintenance of spatial attention. *Neuroimage, 44,* 190–199.

Romei, V., Brodbeck, V., Michel, C., Amedi, A., Pascual-Leone, A., & Thut, G. (2008). Spontaneous fluctuations in posterior alpha-band EEG activity reflect variability in excitability of human visual areas. *Cerebral Cortex, 18,* 2010–2018.

Ruge, H., Brass, M., Koch, I., Rubin, O., Meiran, N., & von Cramon, D. Y. (2005). Advance preparation and stimulus-induced interference in cued task switching: Further insights from BOLD fMRI. *Neuropsychologia, 43,* 340–355.

Rushworth, M. F., Buckley, M. J., Behrens, T. E., Walton, M. E., & Bannerman, D. M. (2007). Functional organization of the medial frontal cortex. *Current Opinion in Neurobiology, 17,* 220–227.

Rushworth, M. F., Paus, T., & Sipila, P. K. (2001). Attention systems and the organization of the human parietal cortex. *Journal of Neuroscience, 21,* 5262–5271.

Shiffrin, R. M., & Schneider, W. (1977). Controlled and automatic human information processing. II. Perceptual learning, automatic attending, and a general theory. *Psychological Review, 84,* 127–190.

Shulman, G. L., Corbetta, M., Buckner, R. L., Raichle, M. E., Fiez, J. A., Miezin, F. M., et al. (1997). Top–down modulation of early sensory cortex. *Cerebral Cortex, 7,* 193–206.

Spierer, L., Murray, M. M., Tardif, E., & Clarke, S. (2008). The path to success in auditory spatial discrimination: Electrical neuroimaging responses within the supratemporal plane predict performance outcome. *Neuroimage, 41,* 493–503.

Spierer, L., Tardif, E., Sperdin, H., Murray, M. M., & Clarke, S. (2007). Learning-induced plasticity in auditory spatial representations revealed by electrical neuroimaging. *Journal of Neuroscience, 27,* 5474–5483.

Spinelli, L., Andino, S. G., Lantz, G., Seeck, M., & Michel, C. M. (2000). Electromagnetic inverse solutions in anatomically constrained spherical head models. *Brain Topography, 13,* 115–125.

Taylor, S. F., Stern, E. R., & Gehring, W. J. (2007). Neural systems for error monitoring: Recent findings and theoretical perspectives. *Neuroscientist, 13,* 160–172.

Thorpe, S. J., & Fabre-Thorpe, M. (2001). Neuroscience. Seeking categories in the brain. *Science, 291,* 260–263.

Thut, G., Nietzel, A., Brandt, S. A., & Pascual-Leone, A. (2006). Alpha-band electroencephalographic activity over occipital cortex indexes visuospatial attention bias and predicts visual target detection. *Journal of Neuroscience, 26,* 9494–9502.

Tibshirani, R., Walther, G., Botstein, D., & Brown, P. (2005). Cluster validation by prediction strength. *Journal of Computational and Graphical Statistics, 14,* 511–528.

Tomasi, D., Ernst, T., Caparelli, E. C., & Chang, L. (2006). Common deactivation patterns during working memory and visual attention tasks: An intra-subject fMRI study at 4 Tesla. *Human Brain Mapping, 27,* 694–705.

Tzourio-Mazoyer, N., Landeau, B., Papathanassiou, D., Crivello, F., Etard, O., Delcroix, N., et al. (2002). Automated anatomical labeling of activations in SPM using a macroscopic anatomical parcellation of the MNI MRI single-subject brain. *Neuroimage, 15,* 273–289.

Tzovara, A., Murray, M. M., Michel, C. M., & De Lucia, M. (in press). A tutorial review of electrical neuroimaging from group-average to single-trial event-related potentials. *Developmental Neuropsychology*.

Ullsperger, M., & von Cramon, D. Y. (2001). Subprocesses of performance monitoring: A dissociation of error processing and response competition revealed by event-related fMRI and ERPs. *Neuroimage, 14,* 1387–1401.

Ullsperger, M., & von Cramon, D. Y. (2004). Neuroimaging of performance monitoring: Error detection and beyond. *Cortex, 40,* 593–604.

Vanderhasselt, M. A., De Raedt, R. R., & Baeken, C. (2009). Dorsolateral prefrontal cortex and Stroop performance: Tackling the lateralization. *Psychonomic Bulletin & Review, 16,* 609–612.

Vanderhasselt, M. A., De Raedt, R., Baeken, C., Leyman, L., & D'haenen, H. (2006). The influence of rTMS over the right dorsolateral prefrontal cortex on intentional set switching. *Experimental Brain Research, 172,* 561–565.

Verbruggen, F., & Logan, G. D. (2008). Automatic and controlled response inhibition: Associative learning in the go/no-go and stop-signal paradigms. *Journal of Experimental Psychology: General, 137,* 649–672.

Vocat, R., Pourtois, G., & Vuilleumier, P. (2008). Unavoidable errors: A spatio-temporal analysis of time-course and neural sources of evoked potentials associated with error processing in a speeded task. *Neuropsychologia, 46,* 2545–2555.

This article has been cited by:

1. Michael De Pretto, Lucien Rochat, Lucas Spierer. 2017. Spatiotemporal brain dynamics supporting the immediate automatization of inhibitory control by implementation intentions. *Scientific Reports* **7**:1. . [Crossref]
2. Andrew Chang, Chien-Chung Chen, Hsin-Hung Li, Chiang-Shan R. Li. 2014. Event-Related Potentials for Post-Error and Post-Conflict Slowing. *PLoS ONE* **9**:6, e99909. [Crossref]
3. Javier SÃ¡nchez-CaÃ±izares. 2014. The role of consciousness in triggering intellectual habits. *Frontiers in Human Neuroscience* **8**. . [Crossref]
4. Etienne Sallard, Jérôme Barral, Camille F. Chavan, Lucas Spierer. 2014. Early attentional processes distinguish selective from global motor inhibitory control: An electrical neuroimaging study. *NeuroImage* **87**, 183-189. [Crossref]
5. Aurelie L. Manuel, Fosco Bernasconi, Lucas Spierer. 2013. Plastic modifications within inhibitory control networks induced by practicing a stop-signal task: An electrical neuroimaging study. *Cortex* **49**:4, 1141-1147. [Crossref]